American Journal of Engineering Research (AJER) ***2018***
American Journal of Engineering Research (AJER)
e-ISSN: 2320-0847 p-ISSN : 2320-0936
Volume-7, Issue-11, pp-158-169
www.ajer.org
Research Paper Open Access

Optimization And Process Modeling Of The Extraction Of Alumina From Aku Clay By Hydrochloric Acid Leaching

Egbuna Samuel Ogbonnaya[1], Mbah Gordian Onyebuchukwu[2], Mbah-Iroulo Ebere Rita[3]
1, 2 & 3 Chemical Engineering Department, Enugu State University of Science and Technology (ESUT), P.M.B. 01660 Enugu, Nigeria
Corresponding Author: Egbuna Samuel Ogbonnaya

ABSTRACT: *The study of extraction of alumina from Aku clay by hydrochloric acid leaching was optimized and modeled. Analysis of the metallic constituents of the clay was carried out using Atomic Absorption Spectrophotometer (AAS). The result of the AAS analysis showed that 31.4739% of alumina is present in the Aku clay. SEM image of the residual clay showed some cracks after the acid leaching buttressing the leaching out of some of its constituents. The study of effect(s) of process variables such as leaching temperature, calcination temperature, acid concentration, liquid-to-solid ratio and contact time was carried out, and further optimized the leaching process using response surface methodology (RSM). The percentage yield obtained at optimal conditions for the leaching of alumina from the Aku clay was 79.4%. The kinetic model of the leaching of alumina from the calcined clay fitted product layer diffusion controlled process with activation energy of 67.98 KJ/mol. The X-ray fluorescence spectrometer analysis showed 94.297 wt% alumina extract.*
KEYWORDS: *Acid leaching, Aku clay, Alumina, Optimization, Hydrochloric acid.*

Date Of Submission:15-11-2018 Date Of Acceptance: 29-11-2018

I. INTRODUCTION

Alumina is a major component of clay. Research studies have shown that clay as a raw material contains about 25–40% of alumina (Ajemba and Onukwuli, 2012). Clays are essentially alumina/silicates which have resulted from weathering of rocks. Some of these clays have weathered under conditions which have concentrated the alumina. These are called high alumina clays. The critical characteristics of alumina/silicates, including clays, as far as treatment to obtain alumina is concerned, is the inherent quality of alumina in its persistent affinity for silica. Because of its affinity for silica, it is difficult to separate alumina from silica and this presents the big problem in treatment of clays (Udeigwe et al., 2015). There are various chemical procedures adopted over the years for the treatment and separation of alumina from clay.

Leaching which is the process of extracting substances from a solid by dissolving them in a liquid has been used through different sintering and acid-extraction processes for the extraction of alumina from clays. The use of some inorganic and organic acids for alumina dissolution (Leaching) have been reported to be feasible, efficient and sustainable (Ajemba & Onukwuli, 2012). Hydrochloric acid has been used by most researchers and it has been found to have some advantages over other acids in terms of alumina production.

However, this study was aimed at the optimization and process modeling of the removal (leaching) of alumina from Aku clay by the use of hydrochloric acid as the leachant.

II. MATERIALS AND METHODS

2.1 Sourcing of Raw materials

The raw clay was collected from "Aku" in Enugu State Eastern Province of Nigeria. The other materials used in the experimental work which included; distilled water, sodium hydroxide and hydrochloric acid was purchased from Ogbete main market Enugu, Nigeria.

2.2 Clay Preparation and Leaching Process

The clay was ground with a laboratory mortar and pestle and sieved to a particle size of 100μm. The Clay was calcined at temperatures between 600˚C and 900˚C .The calcined clay and the raw clay both at 100 μm particle size and 50˚C leaching temperature underwent leaching process by mixing each sample with 3M Hydrochloric acid and 8cm^3 acid/1gm clay liquid to solid weight ratio. The mixture was then stirred at a constant speed of 500 rpm for 60 minutes contact time. After each leaching process, the leached liquor was collected and filtered using Whatman filter paper. 5ml of the filtrate was then withdrawn and analyzed using X-ray Fluorescence (XRF) to determine the amount of alumina present. The experiment was repeated to study the effect of process parameters.

2.3 Extraction of Alumina

Alumina was extracted according to the method of Ajemba and Onukwuli (2012). The filtrate from which iron (III) hydroxide crystallized out was evaporated to dryness and the residue ignited at 1100^{o}C to form alumina (Al_2O_3) and it was weighed. Aluminum ion was confirmed according to the method of (Larson, 2008). The dried residue was dissolved in 0.5M nitric acid. 0.5M barium chloride solution was added in drops, which gave a white precipitate. 1M sodium hydroxide solution was added in drops and warmed with powdered aluminum. The fume given off was tested with damp red litmus paper, which turned the litmus paper blue.

$$\% \text{ Alumina} = \frac{\text{weight of residue}}{\text{theoritcal weight of alumina present in the raw/calcined clay}} \times 100 \qquad (1)$$

2.4 Characterization of the raw and calcine clays

The physical properties of the raw and calcined clay were carried out using ASTM D7263-09(2017) methods. Instrumental of the samples was done using X-Ray Fluorescence (XRF**)** which is controlled by a PC running the dedicated Mini-Pal analytical software. The Mini-Pal 4 version used was PW 4030 X-ray Spectrometer running with voltage (30KV maximum) and a current (1mA maximum) to determine the mineral composition of the clay. Fourier transform infrared spectrometer was used to determine the chemical bond and functional groups in the clay samples. Consequently, Scanning Electron Microscopy (SEM) was used to determine the size and morphology of the clay samples. The SEM micro graph was obtained using JOEL scanning electron microscope model JSM 6400 Scanning electron microscopy recording at 15 KV with 8000x magnification.

2.5 Optimization of leaching process

The optimization of the leaching process was done using Central Composite Design of Response Surface Methodology. Design Expert software (version 9 trial version) was used in this study to design the experiments and to optimize the leaching yield. The experimental design employed in this work was a two-level five factor fractional factorial design, involving 32 experiments. Calcination temperature, Tc, Leaching temperature, TL, acid concentration, A, liquid-solid ratio, LS and contact time, CT were selected as independent factors for the optimization study. The response chosen was the metal yield obtained from leaching of the calcined clay sample. Six replications of centre points were used in order to predict a good estimation of errors and experiments were performed in a randomized order. The actual and coded levels of each factor are shown in Table 2.1. The coded values are designated by −1 (minimum), 0 (centre), +1 (maximum), −α and +α

Table 2.1: Studied range of each factor in actual and coded form.

Independent variables	Symbols	Range and levels				
		-α	-1	0	+1	+α
Calcinations temp. (^{o}C)	A	600	700	800	900	1000
Leaching temp. (^{o}C)	B	30	50	70	90	110
Acid conc. (mol/dm^3)	C	0.75	1.5	2.25	3.0	3.75
Liquid-solid ratio (cm^3/g)	D	4	8	12	16	20
Contact time (min)	E	20	40	60	80	100

Table 2.2: Experimental Design Matrix for Alumina Leaching Process from Aku Clay

Run order	Calcination temperature (°C) A		Leaching temperature (°C) B		Acid concentration (mol/dm^3) C		Liquid-solid ratio (cm^3/g) D		Contact time (min) E	
	Coded	Real	Coded	Real	Coded	Real	Coded	Real	Coded	Real
1	-1	700	-1	50	-1	1.5	-1	8	+1	80
2	+1	900	-1	50	-1	1.5	-1	8	-1	40
3	-1	700	+1	90	-1	1.5	-1	8	-1	40
4	+1	900	+1	90	-1	1.5	-1	8	+1	80
5	-1	700	-1	50	+1	3	-1	8	-1	40
6	+1	900	-1	50	+1	3	-1	8	+1	80
7	-1	700	+1	90	+1	3	-1	8	+1	80
8	+1	900	+1	90	+1	3	-1	8	-1	40
9	-1	700	-1	50	-1	1.5	+1	16	-1	40
10	+1	900	-1	50	-1	1.5	+1	16	+1	80
11	-1	700	+1	90	-1	1.5	+1	16	+1	80
12	+1	900	+1	90	-1	1.5	+1	16	-1	40
13	-1	700	-1	50	+1	3	+1	16	+1	80
14	+1	900	-1	50	+1	3	+1	16	-1	40
15	-1	700	+1	90	+1	3	+1	16	-1	40
16	+1	900	+1	90	+1	3	+1	16	+1	80
17	-2	600	0	70	0	2.25	0	12	0	60
18	+2	1000	0	70	0	2.25	0	12	0	60
19	0	800	-2	30	0	2.25	0	12	0	60
20	0	800	+2	110	0	2.25	0	12	0	60
21	0	800	0	70	-2	0.75	0	12	0	60
22	0	800	0	70	+2	3.75	0	12	0	60
23	0	800	0	70	0	2.25	-2	4	0	60
24	0	800	0	70	0	2.25	+2	20	0	60
25	0	800	0	70	0	2.25	0	12	-2	20
26	0	800	0	70	0	2.25	0	12	+2	100
27	0	800	0	70	0	2.25	0	12	0	60
28	0	800	0	70	0	2.25	0	12	0	60
29	0	800	0	70	0	2.25	0	12	0	60
30	0	800	0	70	0	2.25	0	12	0	60
31	0	800	0	70	0	2.25	0	12	0	60
32	0	800	0	70	0	2.25	0	12	0	60

III. RESULTS AND DISCUSSIONS

3.1 Physico-chemical characterization and properties of the raw and calcined clays

Physcio-chemical properties of the raw and calcined clay are presented in Table 3.1. From the table, it was observed that most of the properties increased after calcination except carbon and organic matter. The porosity was observed to have increased after calcination owing to increase in bulk density (Gray et al., 2014) enabling the leaching solvent to easily permeate the clay and enhance leaching (Onoh et al., 2018).

Table 3.1: Physico-chemical characterization of the clay samples

Sample	pH	Surface Area	Bulk Density (g cm^{-3})	Carbon (%)	Organic Matter (%)	Loss on Ignition (%)	Particle Density (g cm^{-3})	Colour	Total Porosity (%)
Raw Clay	5.66	768.30	1.79	2.03	6.01	9.50	2.33	Light Brown 8/1	23.60
Calcined Clay	7.50	847.15	1.91	1.22	3.63	11.50	3.55	Brownish gray 4/1	46.25

3.2 Atomic Absorption Spectrophotometer (AAS) characterization of the clay samples

AAS results are presented as shown in Table 3.2. It shows the concentration of different elements that are present in the clay samples. From the result, it is observed that the major elements in Aku clay are alumina, iron and sodium while traces of elements such as potassium, manganese, calcium, nickel were also observed. The biggest element in terms of composition in Aku clay was aluminum (Onoh et al., 2018).

Table 3.2: AAS characterization of Aku clay (Onoh et al., 2018)

Elemental Symbol	Aku Clay Concentration (ppm)
Al	31.4739
Fe	26.6340
Na	9.5033
K	0.2833
Mn	0.3203
Ca	0.1314
Ni	0.2067
Mg	0.0325
Cu	0.0264
Zn	0.0180

3.3 Scanning Electron Microscopy (SEM) characterization of virgin and leached clay samples

SEM micrographs of the virgin and leached clay sample are provided in figs 3.1 and 3.2. Fig 3.1 represents the SEM image of the virgin clay 30 m. It was observed from the figure that the clay is a a bulk of microstructure which in turn is composed of a homogeneously distributed network comprised of small filamentous and fistulous crystallites showing the presence of minerals. In the matrix, Luminous and non-luminous features can be seen. These features indicate the presence of minerals distributed in the organic matrix and as surface coverage. Some features such as fissures, cleats, cracks and veins can also be seen. The bright luminosity indicates the presence of lithophytes like magnesium, aluminum, silicon, calcium, titanium etc, and sidrophile, like iron. etiched pits, layers, some islands and hills and valleys can be seen randomly distributed throughout the micrograph. These might be resulted from the calculations of dolomite like $CaMg(C0_3)_2$ and calcites like $CaCO_3$, or their assemblage due to the thermal shock during metamorphism. Some discrete and coherent crystals (framboids, and enthedral) of irregular shapes represent the presence of iron. Veins corresponding to iron oxides can also be seen. It is inferred that Aku clay under study contains large proportions of silica, calcium carbonate as well as some proportions of elements such as aluminum, iron, and potassium (Onoh et al., 2018).

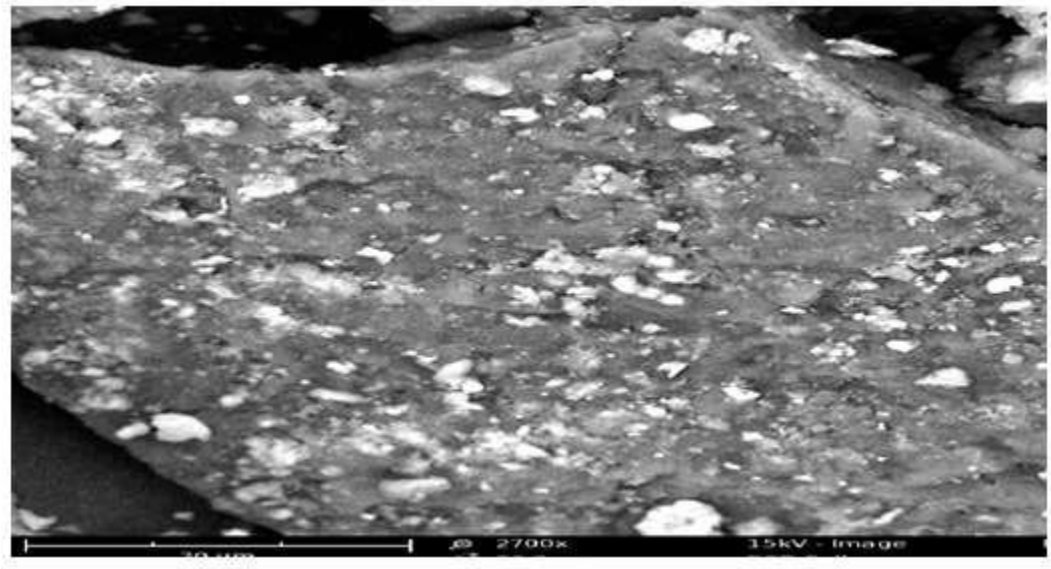

Fig 3.1: SEM image of Aku Virgin clay sample @30µm

It was observed from fig. 3.2 that the porosity increased and provides strong evidence that significant amount of inorganic elements were removed. However the surface coverage is still bright and luminous indicating the presence of mineral phases. It was observed that in the micrograph, the leachant (Conc. HCl) did enormous harm to the surface when compared to the virgin clay. Some minute fissures and cracks, however an evident. The surface was bright and mostly protracted. Some islands can also be seen. However the leachant (HCL) used with the combination of factors for this experiment seem to be effective in leaching of the clay under study (Onoh et al., 2018).

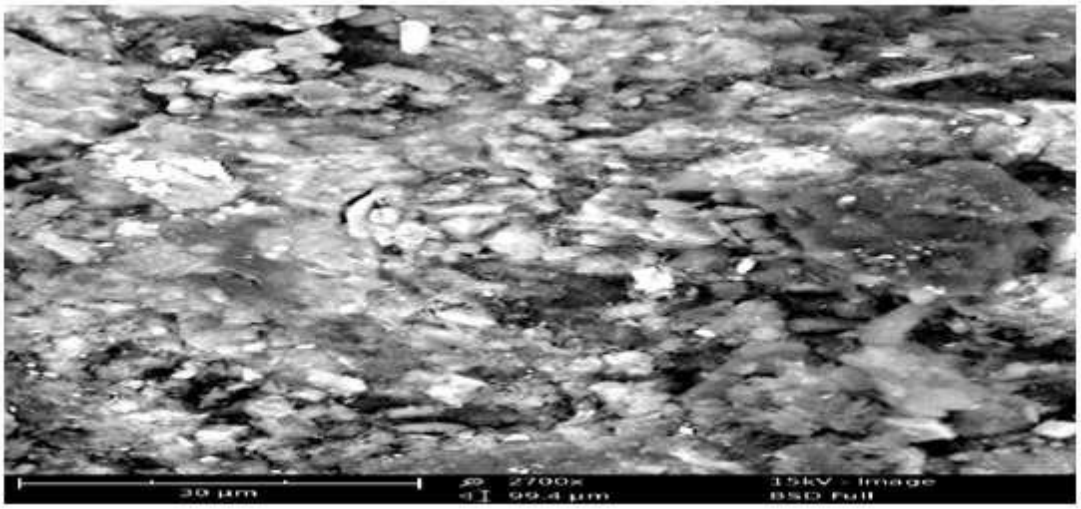

Fig 3.2: SEM image of Leached Clay @ 30µm

3.4 Optimization of leaching of Alumina from 'Aku'clay

To optimize the leaching of alumina, Central Composite Design (CCD) of Response Surface Methodology (RSM) was used to analyze significance of the model and determination of the optimum values of the leaching variables. The actual yields of iron oxide from each experimental run are presented as shown in Table 3.3.

Table 3.3: Yield of alumina using design matrix

Run	A: Calcination temperature ˚C	B: Leaching temperature ˚C.	C: Acid concentration mol/dm^3	D: Liquid-solid ratio ml/g	E: Contact time Minutes	Yield of alumina %
1	700	50	1.5	8	80	48.8
2	900	50	1.5	8	40	61.2
3	700	90	1.5	8	40	52.3
4	900	90	1.5	8	80	59.3
5	700	50	3	8	40	55.6
6	900	50	3	8	80	64
7	700	90	3	8	80	50
8	900	90	3	8	40	57.4
9	700	50	1.5	16	40	66.7
10	900	50	1.5	16	80	66.2
11	700	90	1.5	16	80	61.2
12	900	90	1.5	16	40	56
13	700	50	3	16	80	53.3
14	900	50	3	16	40	65.7
15	700	90	3	16	40	44.3
16	900	90	3	16	80	69.2
17	600	70	2.25	12	60	54.3
18	1000	70	2.25	12	60	69.5
19	800	30	2.25	12	60	65.2
20	800	110	2.25	12	60	58
21	800	70	0.75	12	60	69.5
22	800	70	3.75	12	60	67.4
23	800	70	2.25	4	60	57.3
24	800	70	2.25	20	60	66.7
25	800	70	2.25	12	20	59

26	800	70	2.25	12	100	62
27	800	70	2.25	12	60	79
28	800	70	2.25	12	60	78.3
29	800	70	2.25	12	60	79
30	800	70	2.25	12	60	78.3
31	800	70	2.25	12	60	79
32	800	70	2.25	12	60	78.3

3.5 Analysis of variance (ANOVA) for leaching of alumina

The Analysis of variance of the result of the experiments in table 3.3 was carried out. The percentage yield of iron oxide extracted depends on the results if the interaction between the process parameters is significant.

Using the same Design expert version 9.0.7.1, Equation 2 was obtained as the quadratic equation that fitted the data.

$$Y_{alumina} = 78.79 + 4.05A - 1.92B - 0.68C + 2.20D + 0.78E + 2.46AC + 1.5AE - 0.22BC - 0.66BD + 2.91BE - 1.44CD + 0.89CE + 1.35DE - 4.32A^2 - 4.40B^2 - 2.69C^2 - 4.30D^2 - 4.67E^2 \quad (2)$$

Table 3.5: Analysis of variance table for the yield of alumina

Source	Coefficient estimate	Degree of freedom	Sum of square	Mean Square	F-value	P-value (Prob >F)
Model	78.79	20	2884.99	144.25	336.80	< 0.0001
A	4.05	1	393.66	393.66	919.14	<0.0001
B	-1.92	1	88.94	88.94	207.65	< 0.0001
C	-0.68	1	11.21	11.21	26.17	0.0003
D	2.20	1	116.16	116.16	271.22	< 0.0001
E	0.78	1	14.73	14.73	34.38	0.0001
AC	2.46	1	97.02	97.02	226.53	< 0.0001
AE	1.50	1	36.00	36.00	84.05	0.0019
BC	-0.22	1	0.81	0.81	1.89	<0.0001
BD	-0.66	1	7.02	7.02	16.40	< 0.0001
BE	2.91	1	135.72	135.72	316.89	< 0.0001
CD	-1.44	1	33.06	33.06	77.20	<0.0001
CE	0.89	1	12.60	12.60	29.43	0.0002
DE	1.35	1	29.16	29.16	68.08	<0.0001
A^2	-4.32	1	548.41	548.60	1280.46	< 0.0001
B^2	-4.40	1	567.60	567.60	1325.26	< 0.0001
C^2	-2.69	1	211.69	211.69	494.25	< 0.0001
D^2	-4.30	1	542.09	542.09	1265.69	< 0.0001
E^2	-4.67	1	640.79	640.79	1496.14	< 0.0001
Residual			**0.43**			
Cor. Total			**2889.70**			

Std. Dev. = 0.65; Mean = 63.50; C.V.% = 1.03; PRESS = 97.96; R^2 = 0.9984; Adj. R^2 = 0.9954; Pred. R^2 = 0.9661; Adeq. Precision = 63.988

The ANOVA results for the model terms are given in Table 3.4. Analysis of variance (ANOVA) was applied for estimating the significance of the model at 5% significance level and shown in Table 3.4. A model is considered significant if the p-value (significance probability value) is less than 0.05. From the p-values presented in Table 4.5, it can be deduced that all the linear terms A, B, C, D and E and interaction terms AC, AE, BD, BE, CD, CE, DE and quadratic terms A^2, B^2, C^2, D^2, and E^2 were significant model terms. Based on this, the insignificant terms (AB and AD) of the model were removed and the model reduced to the following equation:

$$Y_{alumina} = 78.79 + 4.05A - 1.92B - 0.68C + 2.20D + 0.78E + 2.46AC + 1.5AE - 0.22BC - 0.66BD + 2.91BE - 1.44CD + 0.89CE + 1.35DE - 4.32A^2 - 4.40B^2 - 2.69C^2 - 4.30D^2 - 4.67E^2 \quad (3)$$

The experimental data in Table 3.3 were also analyzed to check the correlation between the experimental and predicted alumina yield. The normal probability versus residual plot, and actual versus predicted plot are shown in Figs. 3.3 and 3.4 respectively. It can be seen from the Figures that the data points on the plot were reasonably distributed near to the straight line, indicating a good relationship between the experimental and predicted values of the response, and that the underlying assumptions of the above analysis

were appropriate. The result also suggests that the selected quadratic model was adequate in predicting the response variables for the experimental data.

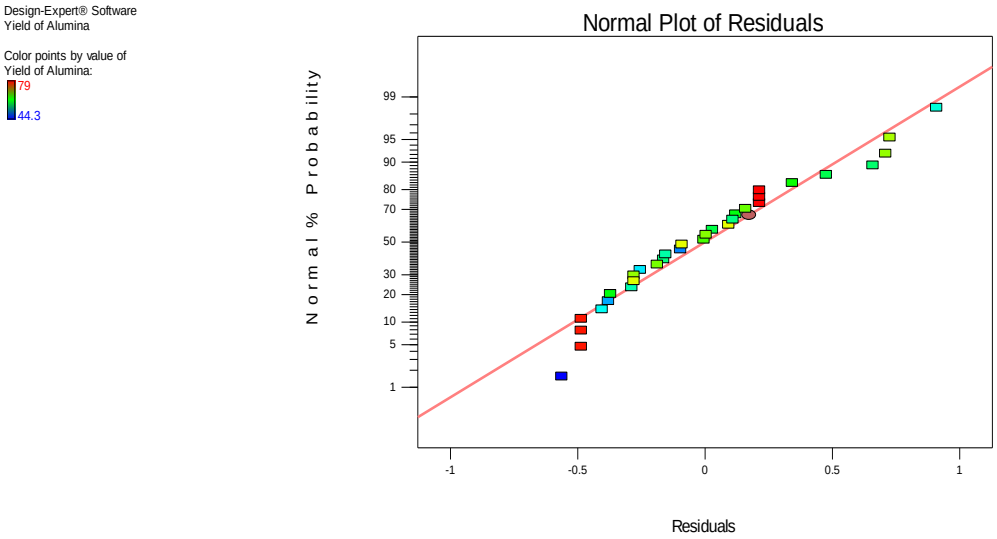

Fig 3.3: Plot of normal probability versus residuals alumina yield.

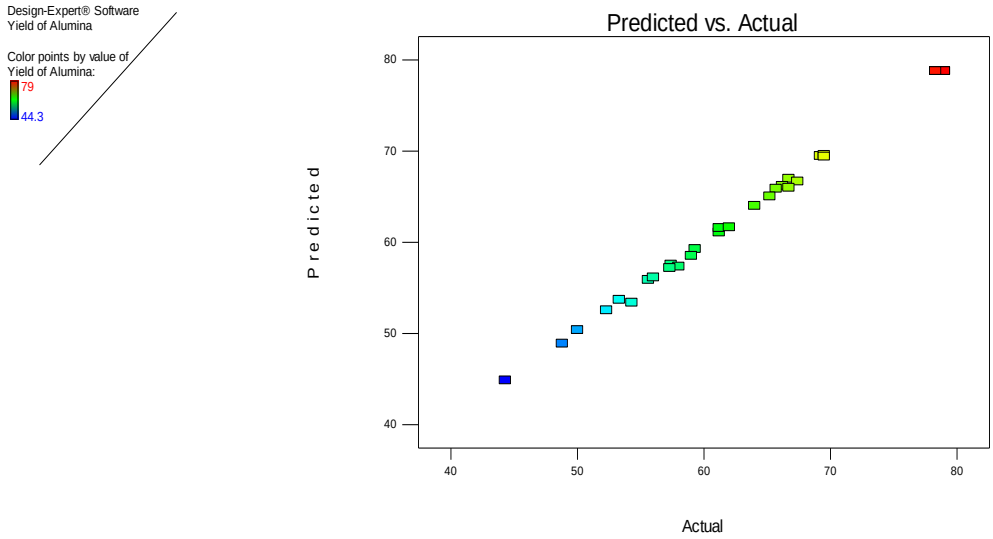

Fig 3.4: Plot of predicted versus actual alumina yield.

3.6 Surface Plots for alumina yield

The 3D response surface was generated to estimate the effect of the combinations of the independent variables on the alumina yield. The plots are shown in Figs. 3.5 to 3.12. Fig. 3.5 shows the dependency of alumina yield on the interaction of calcination temperature and acid concentration. As can be seen from the Fig 3.5, percentage alumina yield increases as both the calcination temperature and acid concentration increase up to the mid point of these variables and then decreased for acid concentration and remained constant for calcination temperature. This could be due to total dehydration and solid-phase transformation of alumina at mid point of the variables and sintering effect at high temperature.

Fig. 3.6 shows the dependency of alumina yield on calcination temperature and contact time. As can be seen from the figure, percentage alumina yield increases as both the calcination temperature and contact time increases up to the mid point of these variables and then decreased beyond 65 minutes contact time and 850^{o}C calcination temperature. This may be that the alumina present has been extracted at contact time of 65 minutes and due to sintering effect at high temperature.

Fig 3.7 shows the dependency of alumina yield on leaching temperature and acid concentration. As can be seen from the figure, percentage alumina yield increases as both the leaching temperature and acid

concentration increase up to the mid point of these variables and then decreased. This may be that beyond the midpoints of these variables, the conditions were no longer favorable for leaching because higher acid concentration and temperature.

Fig 3.8 shows the dependency of alumina yield on leaching temperature and liquid to solid ratio. As can be seen from the figure, percentage alumina yield increases as both the leaching temperature and liquid to solid ratio increase up to the mid point of these variables and then decreased. This may be that beyond the midpoints of these variables, the conditions were no longer favorable for leaching as a result of high temeprature.

Fig 3.9 shows the dependency of alumina yield on leaching temperature and contact time. As can be seen from the figure, percentage alumina yield increases as both the leaching temperature and contact time increased up to the mid point of these variables and then decreased. This may be attributed to unfavorable conditions for leaching beyond the midpoints of these variables.

Fig 3.10 shows the dependency of alumina yield on acid concentration and liquid to solid ratio. As can be seen from the figure, percentage alumina yield increases as both the acid concentration and liquid to solid ratio increased up to the mid point of these variables and then decreased. This may be that beyond the midpoints of these variables, the conditions were no longer favourable for leaching because of high acid concentration.

Fig 3.11 shows the dependency of alumina yield on acid concentration and contact time. As can be seen from the figure, percentage alumina yield increases as both the acid concentration and contact time increased up to the mid point of these variables and then decreased. This could be that beyond the midpoints of these variables, the conditions were no longer favorable for leaching because the metals have been leached out before the longer time could be reached.

Fig 3.12 shows the dependency of alumina yield on contact time and liquid to solid ratio. As can be seen from the figure, percentage alumina yield increases as both the contact time and liquid to solid ratio increased up to the mid point of these variables and then decreased. This could be that beyond the midpoints of these variables, the conditions were no longer favorable for leaching.

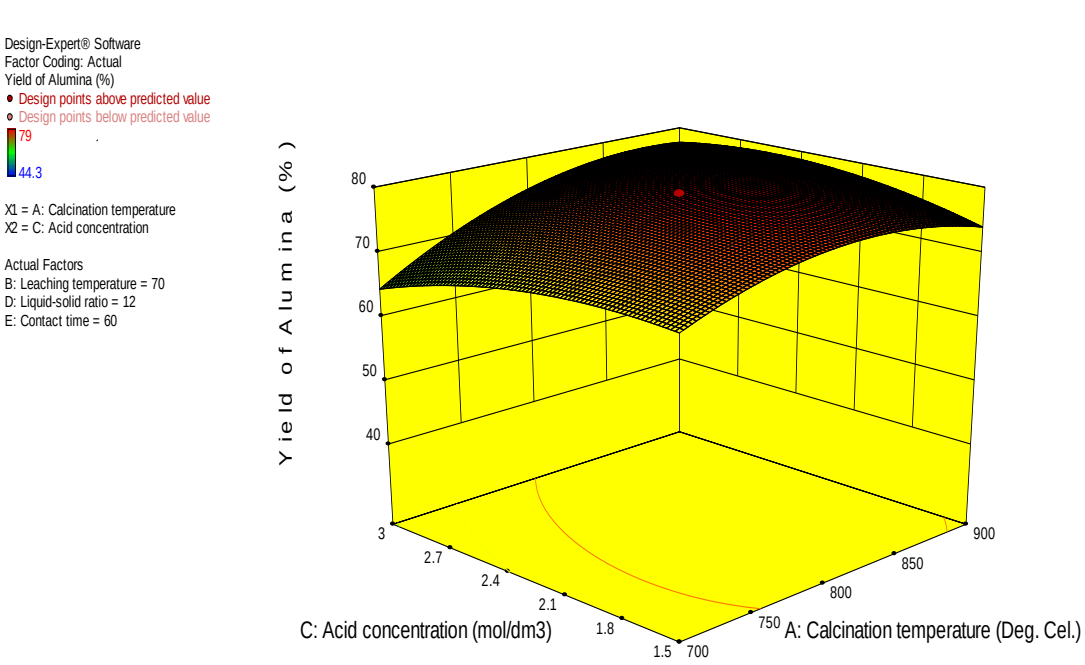

Fig 3.5: 3D plots showing the effect of calcination temperature and acid concentration on the alumina yield

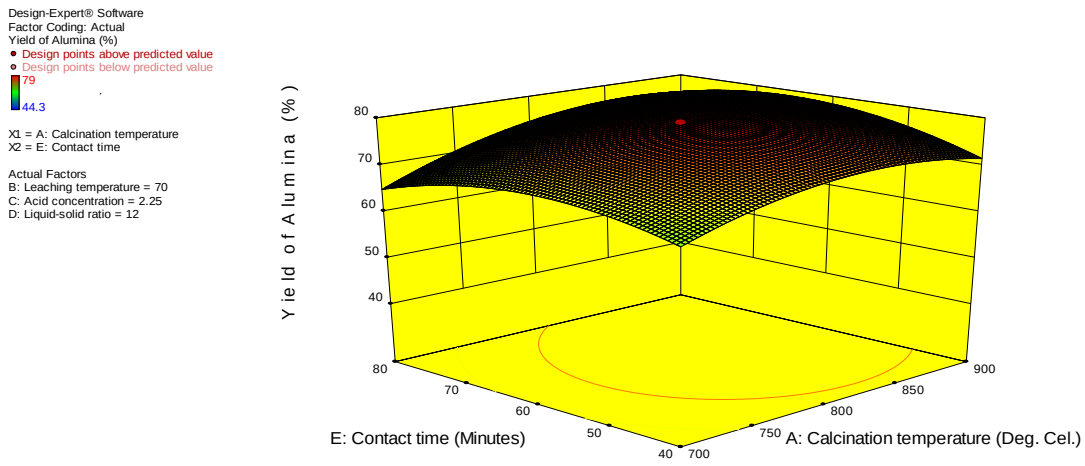

Fig 3.6: 3D plots showing the effect of calcination temperature and contact time on the alumina yield

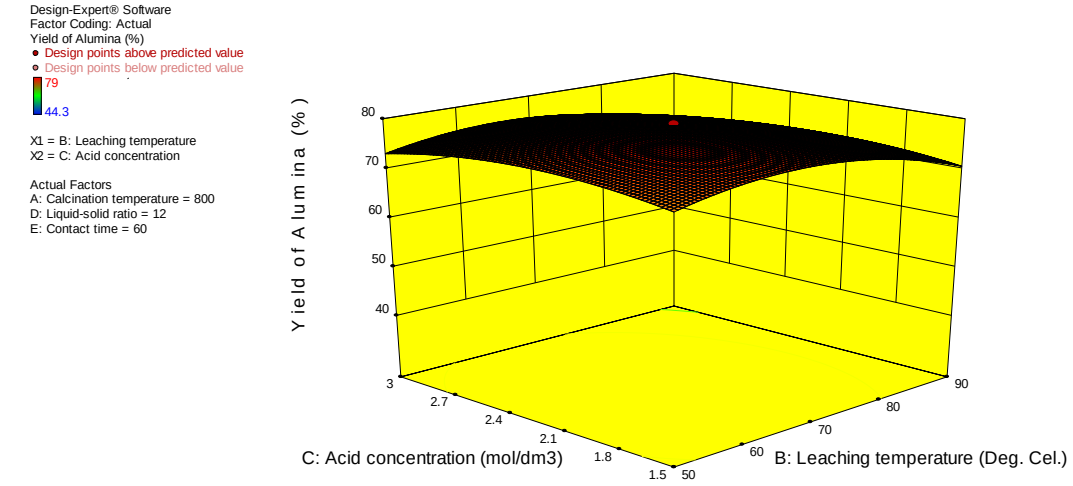

Fig 3.7: 3D plots showing the effect of leaching temperature and acid concentration on the alumina yield

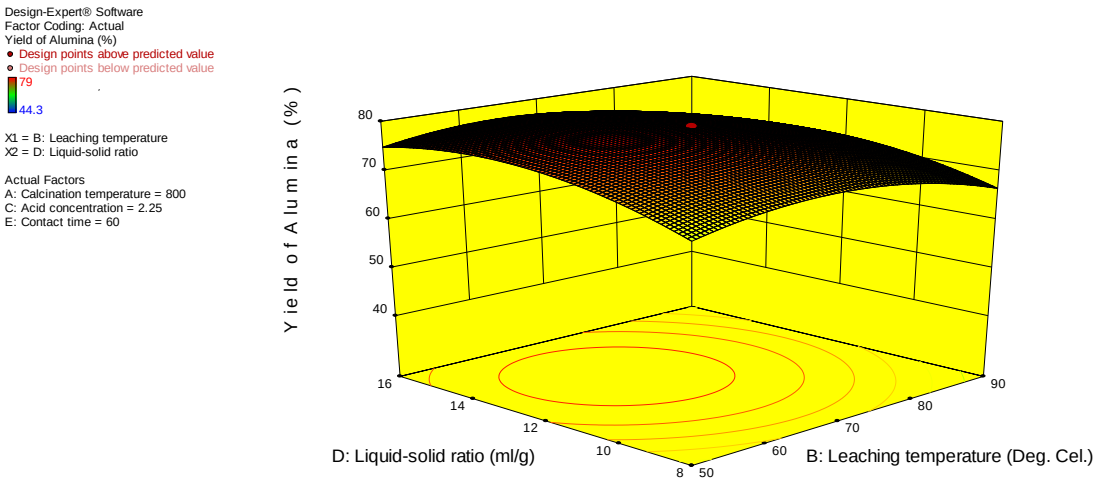

Fig 3.8: 3D plots showing the effect of leaching temperature and liquid to solid ratio on the alumina yield

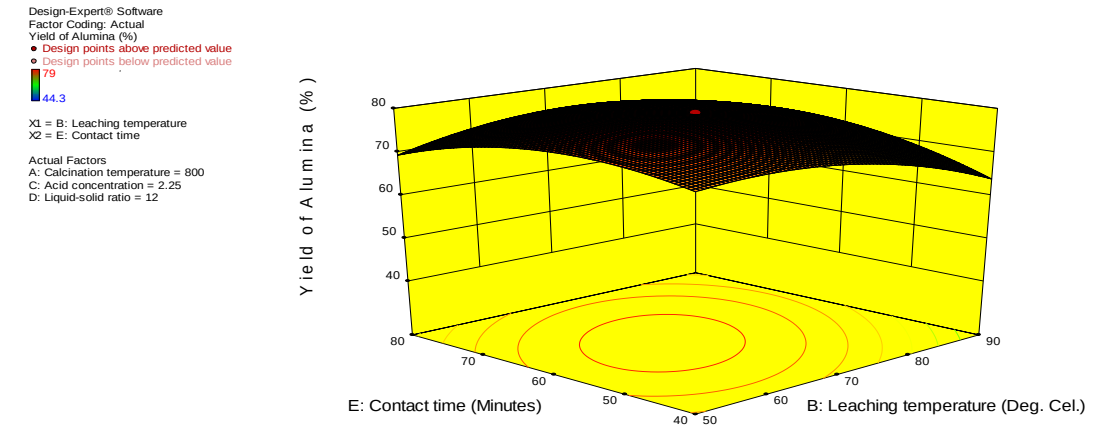

Fig 3.9: 3D plots showing the effect of leaching temperature and contact time on the alumina yield

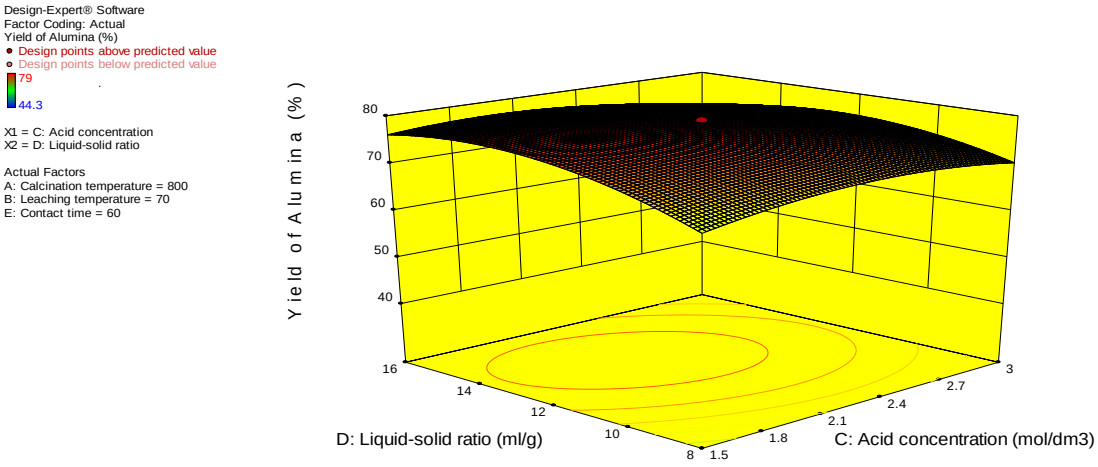

Fig 3.10: 3D plots showing the effect of acid concentration and liquid to solid ratio on the alumina yield

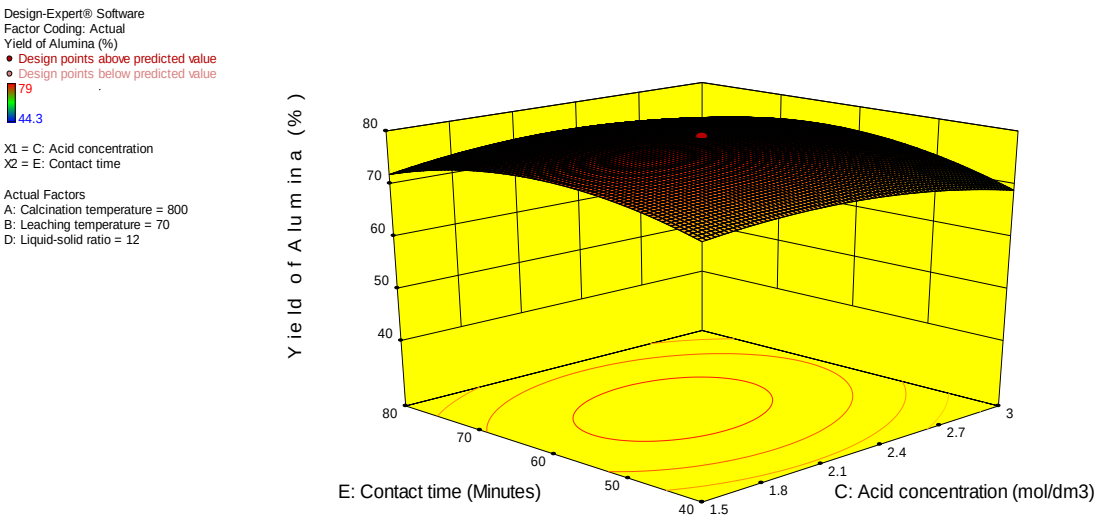

Fig 3.11: 3D plots showing the effect of acid concentration and contact time on the alumina yield

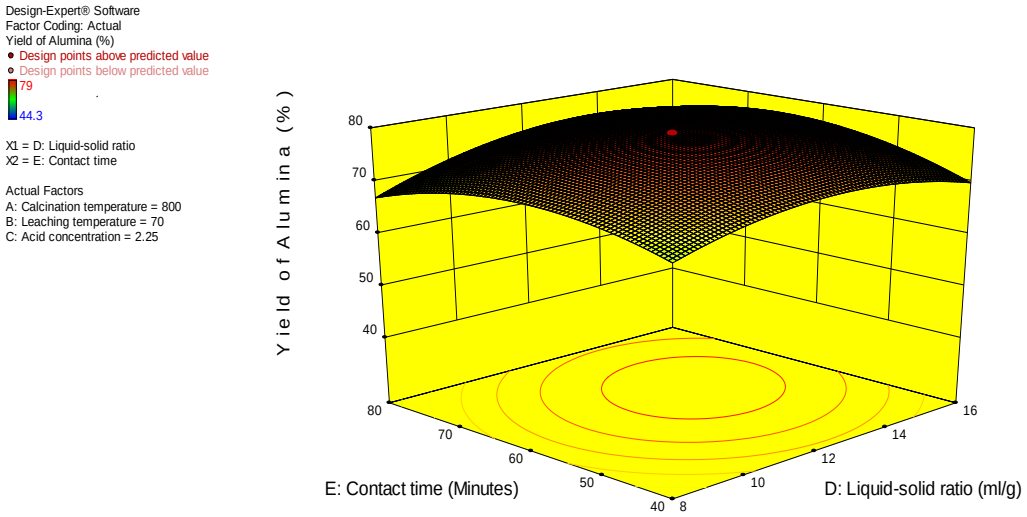

Fig 3.12: 3D plots showing the effect of contact time and liquid to solid ratio on the alumina yield

Table 3.5: Predicted and Experimental values for alumina

Calcination temperature (^oC)	Leaching temperature (^oC)	Acid concentration (mol/dm^3)	Liquid to solid ratio (ml/g)	Contact time (Minutes)	Experimental Yield (%)	Predicted yield (%)
820	67	2.2	12.9	61	78.4	79.98

The leaching of alumina under the obtained optimum operating conditions was carried out in order to evaluate the precision of the quadratic model; the experimental value and predicted values are shown in Table 3.5 above. Comparing the experimental and predicted results, it is observed that the error between the experimental and predicted value is less than 3%, therefore it can be concluded that the generated model has sufficient accurancy to predict the alumina yield.

3.7 PERCENTAGE OF ALUMINA IN THE EXTRACT

The leached extract/sample was characterized with X-Ray fluorescence spectrometer and the result presented in Table 3.6. From the table, it could be observed that percentage alumina in the metallic oxide is 94.297 wt%. This shows that alumina was extracted but requires further purification.

Table 3.6: Percentage composition of the leached extract

Element	Concentration (wt%)
Na_2O	0.745
MgO	0.796
Al_2O_3	94.297
SiO_2	3.70
P_2O_5	0.010
SO_3	0.117
Cl	0.213
K_2O	0.012
CaO	0.075
TiO_2	0.004
Cr_2O_3	0.00
Mn_2O_3	0.003
Fe_2O_3	0.027
ZnO	0.002
SrO	0.000

REFERENCES

[1]. Ajemba, R., Onukwuli O. Process Optimization of Sulphuric acid Leaching of Alumina from Nteje Clay using Central Composite Rotatable Design: International Journal of Multidisciplinary sciences and Engineering, 3(5), (2012) 116-121.
[2]. Ajemba, R.O., Onukwuli, O.D. Kinetic Model for Ukpor Clay Dissolution in Hydrochloric acid solution: Journal of Emerging Trends in Engineering and Applied Sciences. 3 (3): (2012) 448-454.
[3]. ASTM D7263-09. Standard Test Methods for Laboratory Determination of Density (Unit Weight) of Soil Specimens, ASTM International, West Conshohocken, PA, 2017, www.astm.org accessed October, 2017.
[4]. Gray, M., Johnson, M. G., Dragila, M. I., & Kleber, M. Water uptake in biochars: The roles of porosity and hydrophobicity. Biomass and Bioenergy, 61, (2014) 196-205. doi:10.1016/j.biombioe.2013.12.010.
[5]. Larson, L.J. (2008). Seperation and Identification of Group B Cations. Foothill College Chemistry I C. pp:2.
[6]. Madejová, J., (2003). FTIR techniques in clay mineral studies. Vibrational Spectroscopy, 31 (1), 1 – 10.
[7]. Olaremu, A. G. (2015). Sequential leaching for the production of alumina from a Nigerian clay. International Journal of Engineering Technology, Management and Applied Sciences, 3(7), 103 -109.
[8]. Ozdemir, M., Cetisli, H. (2005). Extraction kinetics of alumina in sulphuric acid and hydrochloric acid. Hydrometallurgy, 76(3-4), 217-224.
[9]. Sultana, U. K., Gulshan, F., Gafur, M. A., Kurny, A. S. W., (2013). Kinetics of recovery of alumina from aluminium casting waste through fusion with sodium hydroxide. American Journal of Materials Engineering and Technology, 1(3), 30-34.
[10]. Udeigwe U., Onukwuli, O. D., Ajemba R., Ude C. N. (2015). Kinetics studies of hydrochloric acid leaching of alumina from Agbaja clay. International Journal of Research in Advanced Engineering and Technology, 1(1), 64-72.
[11]. Udeigwe U., Onukwuli, O. D., Ajemba R., Ude C. N. Kinetics studies of hydrochloric acid leaching of alumina from Agbaja clay. International Journal of Research in Advanced Engineering and Technology, 1(1), (2015) 64-72.
[12]. Willis, R. D., Blanchard, F. T. & Connor, T. L. (2002). Guidelines for the Application of SEM/EDX Analytical Techniques to Particulate Matter Samples. U.S. Environmental Protection Agency #600/R-02/070.